ION-SOUND MODEL OF MICROWAVE SPIKES WITH FAST SHOCKS IN THE RECONNECTION REGION

G. P. CHERNOV[1], Q. J. FU[2], D. B. LAO[2] and Y. HANAOKA[3]
[1] *IZMIRAN, Troitsk, Moscow Region, 142092, Russia*
[2] *BAO, Beijing, Chinese Academy of Sciences, 100080, China*
[3] *National Astronomical Observatory of Japan, Tokyo*

(Received 18 January 2000; accepted 12 January 2001)

Abstract. A new model for solar spike bursts is considered based on the interaction of Langmuir waves with ion-sound waves: $l + s \rightarrow t$. Such a mechanism can operate in shock fronts, propagating from a magnetic reconnection region. New observations of microwave millisecond spikes are discussed. They have been observed in two events: 4 November 1997 between 05:52–06:10 UT and 28 November 1997 between 05:00–05:10 UT using the multichannel spectrograph in the range 2.6–3.8 GHz of Beijing AO. *Yohkoh*/SXT images in the AR and SOHO EIT images testify to a reconstruction of bright loops after the escape of a CME. A fast shock front might be manifested as a very bright line in T_e SXT maps (up to 20 MK) above dense structures in emission measure (*EM*) maps. Moreover one can see at the moment of spike emission (for the 28 November 1997 event) an additional maximum at the loop top on the HXR map in the AR as principal evidence of fast shock propagation. The model gives the ordinary mode of spike emission. Sometimes we observed a different polarization of microwave spikes that might be connected with the depolarization of the emission in the transverse magnetic field and rather in the vanishing magnetic field in the middle of the QT region. Duration and frequency band of isolated spikes are connected with parameters of fast particle beams and shock front. Millisecond microwave spikes are probably a unique manifestation of flare fast shocks in the radio emission.

1. Introduction

Spikes are a well-known structure in the solar radio emission since 1961 at frequencies around 0.3 GHz owing to almost simultaneous observations by Dröge and Rieman, Elgarøy, and de Groot (see a review by Benz, 1993). Later they received little attention and only one theoretical paper by Zheleznyakov and Zaitsev (1975), regarding a plasma emission mechanism for spikes at the starting frequencies of type III bursts.

But since 1978, when C. Slottje had observed millisecond spikes at 2.695 GHz, they have attracted considerable attention. They have been identified by spectrometers in the 0.3–8 GHz range as narrowband spikes (Benz, 1986, 1993).

The theory of electron cyclotron maser instability (ECMI) seemed to be the most attractive model to account for the main properties of millisecond spikes (Melrose and Dulk, 1982; Wu, 1985; Aschwanden, 1990; Fleishman and Mel'nikov,

Solar Physics **201:** 153–180, 2001.

1998, and references therein). Quasilinear simulations of Aschwanden (1990) are a culmination of such a model.

However, dissatisfaction remains, connected with some essential results: only X and Z magnetoionic modes can mainly be emitted by ECMI in a region where the ratio of electron plasma and cyclotron frequencies $\omega_{\mathrm{Pe}}/\omega_{\mathrm{Be}} < 0.5$, meaning very strong magnetic field (B) at heights $> 10^4$ km, and emission frequency $\omega \approx \omega_{\mathrm{Be}}$, i.e., $B \approx 1000$ G at plasma levels $f_{\mathrm{Pe}} \approx 3000$ MHz.

At the same time all previous optical observations and 3-dimensional simulations of magnetic fields in the corona show significantly smaller values of B (Rubin, 1997).

According to the results of Krucker, Benz, and Aschwanden (1997) sources of spikes at 333 MHz were located high in the corona ($h \approx 5 \times 10^{10}$ km) and were probably connected with a high coronal flare and emitted by the plasma mechanism of Zheleznykov and Zaitsev (1975) in the ordinary magnetoionic mode. However, in Benz and Güdel (1987), Krucker *et al.* (1995a) and Güdel and Zlobec (1991) we have the opposite information concerning the magnetoionic mode.

In the meter wave range spikes are often observed in noise storms and in the type IV continuum without connection with type III bursts as proposed in the model of Zheleznyakov and Zaitsev (1975).

Decimeter spikes occur during the impulsive phase of flares and often correlate with hard X-ray emission (Aschwanden and Güdel, 1992) but meter spikes have only a small simultaneous increase of *Yohkoh*/SXR emission (Krucker *et al.*, 1995a).

Microwave millisecond spikes more often have a small polarization degree (see Alaart *et al.*, 1990) in contradiction with the model of ECMI, unless the polarization is decreased or reversed during propagation through a transverse magnetic field. For microwave spikes we do not have so far any exact information about source positions and magnetic field polarity.

Thus the open questions are the wave modes and moderate polarization degrees of spikes in different frequency ranges. Spikes in the meter range and at microwaves may be of course of a different nature, since first of all, for metric spikes, the brightness temperature has an observed $T_b \approx 3 \times 10^6$ K. However, the last value is rather underestimated in connection with a broadening of the source size due to the scattering of radio emission in the solar corona. In the decimeter and microwave ranges T_b is usually proposed as $\geq 10^{14}$–10^{15} K.

Between 1000 and 2000 MHz a structure like the harmonic bands of spikes was observed (Güdel and Benz, 1990) with a proposed harmonic number $s = 2$–6. Such observations yield a new difficulty for the spike interpretation.

The main problems with ECMI are the escape of the radiation through the outer corona without absorption (at the third cyclotron level) and the low-plasma beta, which is required for the growth of maser instability.

To avoid some difficulties Wang and Li (1991) proposed a model of nonlinear parametric instability for millisecond spikes. But excepting definitive difficulties

with the carrying-out of the matching conditions for the coupling process of two electromagnetic waves with a whistler wave, the pump electromagnetic wave must be strong for the nonlinear parametric instability. It should propose also enough rare conditions high in the solar corona for a whistler instability with very small whistler wave numbers $k_w \ll \omega_{\mathrm{Pe}}/c$. Moreover, such a model can explain only strictly periodic spikes.

The solution of the nonlinear Schrödinger equation for the pump wave in Wang and Li (1991) with consideration of the Miller force (ponderomotive force in the equation of electron motion) contradicts the conclusion of Wentzel and Aschwanden (1991): the maximum energy density inferred in the spike emission by ECMI is at least two order of magnitude less than the energy density at which electron entrainment sets in. The ECMI is a phenomenon described instead in the quasilinear regime (simulations of Aschwanden, 1990).

Thus we have no well-accepted emission mechanism to explain the main spike parameters in the meter and decimeter range unlike for microwaves. Although there is general agreement that the emission mechanism has to be coherent, it remains unclear whether it is by gyroemission or plasma emission as proposed by Altyntsev, Grechnev, and Hanaoka (1998). New simultaneous positional observations in the radio range (with spectrum and polarization) together with optical and X-ray images are needed. At the same time recent *Yohkoh* data testify about fast shock fronts in the flare region during magnetic reconnection at X-points (Tsuneta, 1996).

In the metric range fast shocks are the source of the most spectacular radio bursts of type II. At microwaves the connection of any radio details with flare fast shocks is unknown up to now, although in shock fronts plasma wave turbulence develops. We propose that the propagation of fast fronts through the microwave source could generate additional fast bursts of spikes.

In this paper we present new observations of millisecond spikes and discuss them using a model of spike emission due to the coalescence of Langmuir waves with ion-sound waves in a source connected with fast shock fronts in the reconnection region. We think that millisecond microwave spikes are a unique manifestation of flare fast shocks in the radio emission.

The structure of this paper is as follows: in Section 2 new observations are presented and discussed; Section 3 is devoted to the short description of a new source model; Section 4 contains the analysis of the interaction $l + s \rightarrow t$ and presents the interpretation of physical parameters deduced from this process; a summary and conclusions are given in Section 5.

2. New Observations

For a detailed study of the problems mentioned above new observations of intensity and polarization with high resolution in time and in frequency in decimeter and microwave wavebands are essential. In order to investigate these features in great

detail, the new multichannel microwave spectrometer of BAO was used (Fu *et al.*, 1995). One hundred and twenty-eight channels provide high-frequency (10 MHz) and high-time (8 ms) resolution with high sensitivity and high accuracy measures of circular polarization. The 4 November 1997 event is the more intense one and the 28 November 1997 is the more meaningful one with spikes from five events with spikes.

2.1. 4 AND 28 NOVEMBER 1997 EVENTS

2.1.1. *Radio Data*

The big radio burst was observed in 4 November 1997 between 05:52–06:10 UT. It may be classified as the type GRF with maximal flux at 3000 MHz ($\sim$ 1500 sfu). Multichannel time profiles between 2.73–3.77 GHz from the spectrometer of BAO are shown at the Figure 1(a).

The event was connected with a big Hα flare (importance 2B X2.1) in NOAA AR8100 (S14 W33) between 05:54 and 07:15 UT. At the Culgoora radio spectrum in the frequency range 18–1800 MHz it was classified as a big type II+IV burst.

The event of 28 November 1997 was connected with a 2B M6.8 flare (04:56–06:33 UT) near the east limb (AR 8113, N15 E61) but the radio burst was more than three times weaker. Time profiles are shown in Figure 1(b).

Multichannel radio time profiles of both events received with the spectrometer of BAO in the range 2.6–3.8 GHz reveal a good correlation with the BATSE HXR profile (23.7–65.4 keV). At the beginning of the burst of 4 November (at 05:57:30 UT) the emission changed polarization sign from right to left, practically simultaneously at all frequencies (bottom of Figure 2(a)). During the 28 November event the polarization changed sign five times with a periodicity of $\leq$ 1 min (bottom of Figure 2(b)).

Spikes were observed only during some seconds at some frequency channels at the post-maximum phase of the bursts of 4 and 28 November 1997. Figures 3(a) and 3(b) show millisecond spikes with high-time resolution. At the top of Figure 3(a) we can see spike profiles in total intensity (s.f.u.). The duration of each spike is at the 8 ms limit of the instrument time resolution. Spikes are visible in only one polarization channel (middle parts of Figures 3(a) and 3(b)), i.e., the spike emission is fully polarized. In the dynamic spectrum each spike is visible only in one pixel (bottom of Figure 3(b)), i.e., their frequency bandwidth $\leq$ 10–20 MHz ($\Delta f/f \leq 0.007$).

Another peculiarity visible in the left polarization channels in Figure 3(a) is a weak diffuse background emission around spikes with a maximal duration of about 80 ms and a remarkable positive frequency drift at about 1 GHz s^{-1}.

Millisecond spikes were observed also in three other events and the main parameters of five events with spikes are summarized in Table I.

For the event of 14 May 1993 the position of spike sources was well defined by Nobeyama 17 GHz and *Yohkoh*/SXT data. For the events of 25 November 1996

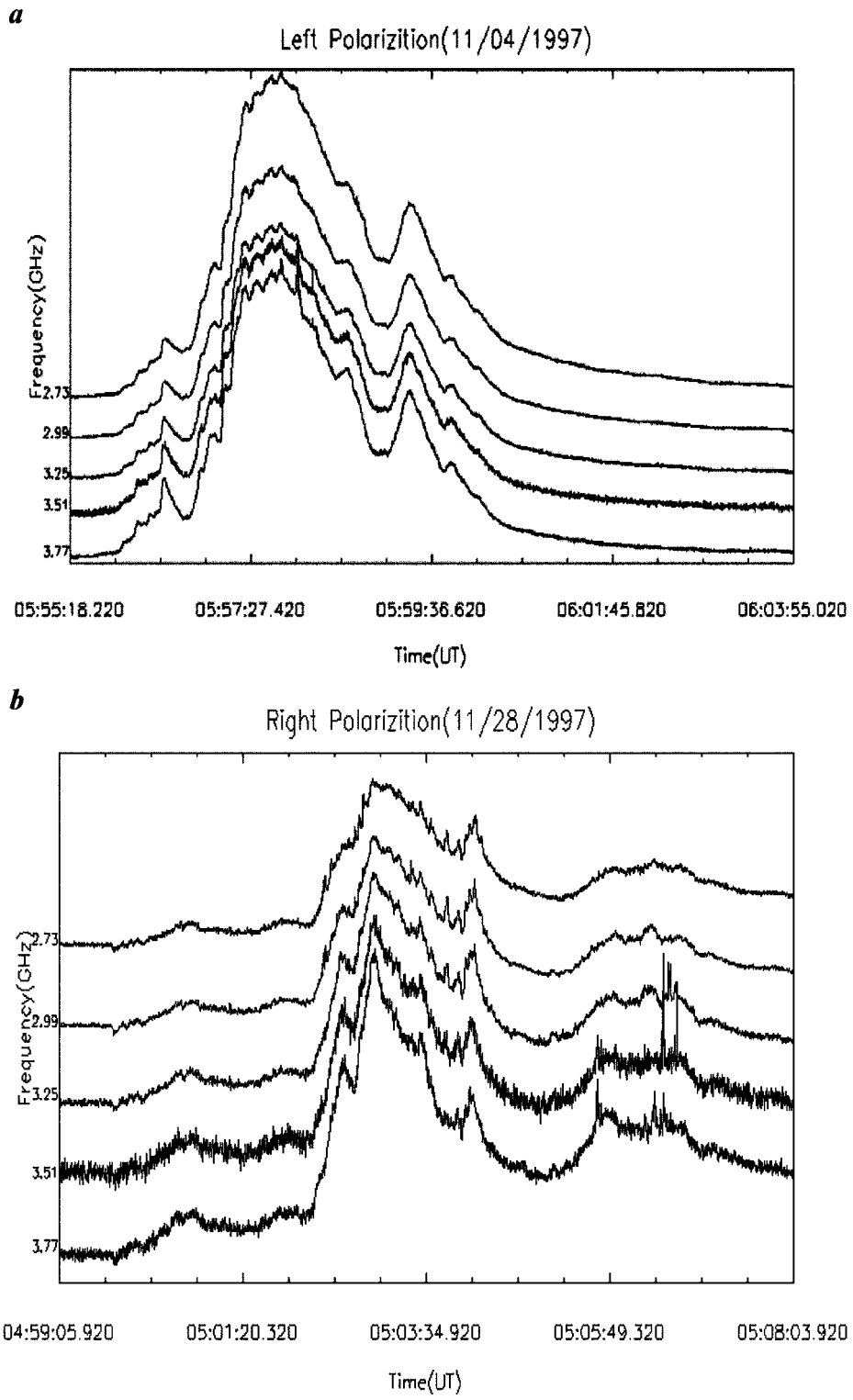

Figure 1. (a) The event of 4 November 1997 as it was seen by microwave spectrograph between 2.6–3.8 GHz at Beijing Astronomical Observatory in multichannel profile presentation. (b) Similar data for the event of 28 November 1997.

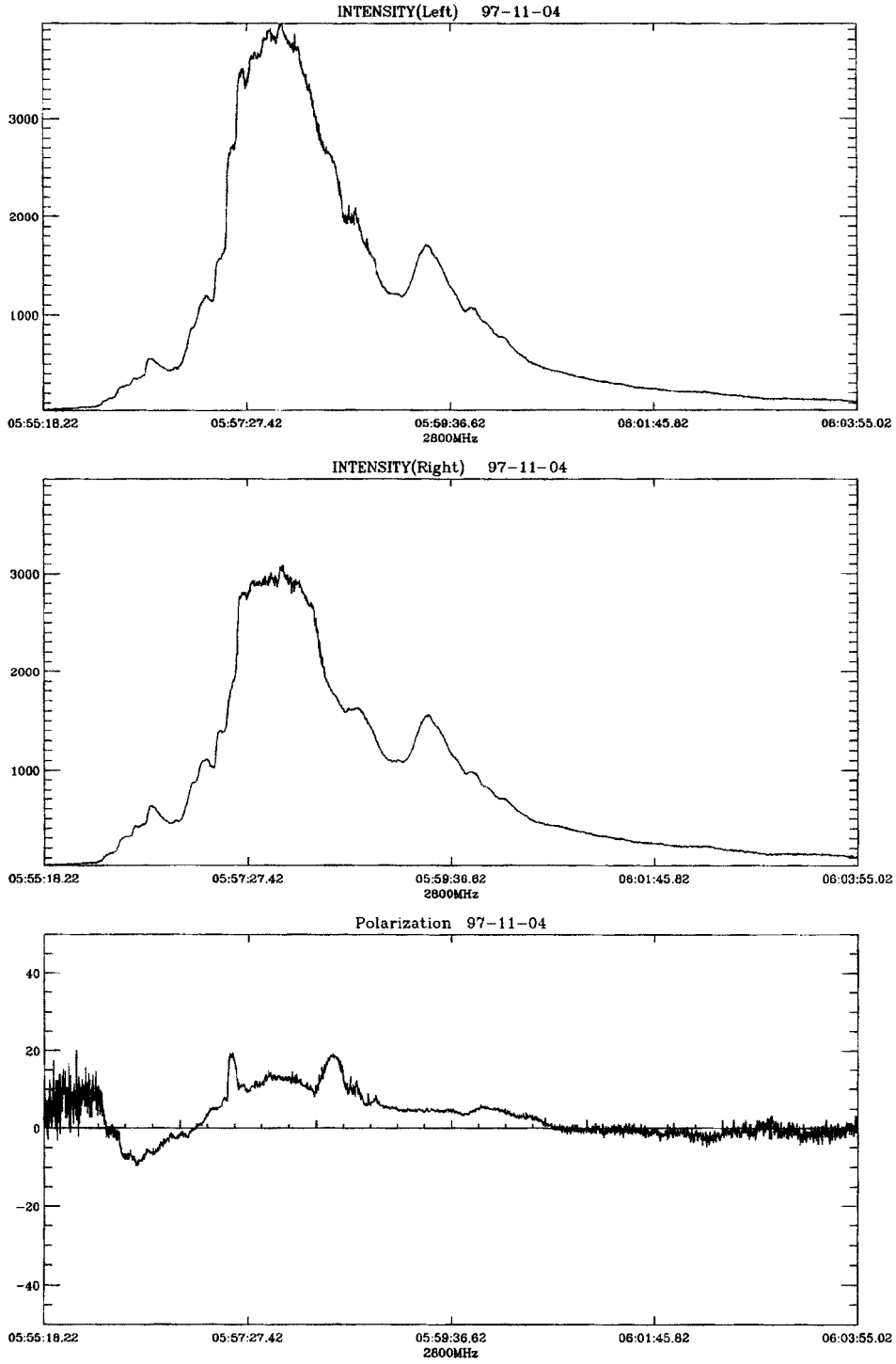

Figure 2a.

Figure 2. (a) LCP, RCP and net polarization profiles at 2800 MHz on 4 November 1997. The polarization changed sign (from right to left) in the beginning of the event (practically simultaneously at all frequencies) near 05:57 UT. (b) Similar profiles for the event 28 November 1997 at 3160 MHz. The polarization changed sign 5 times during the event.

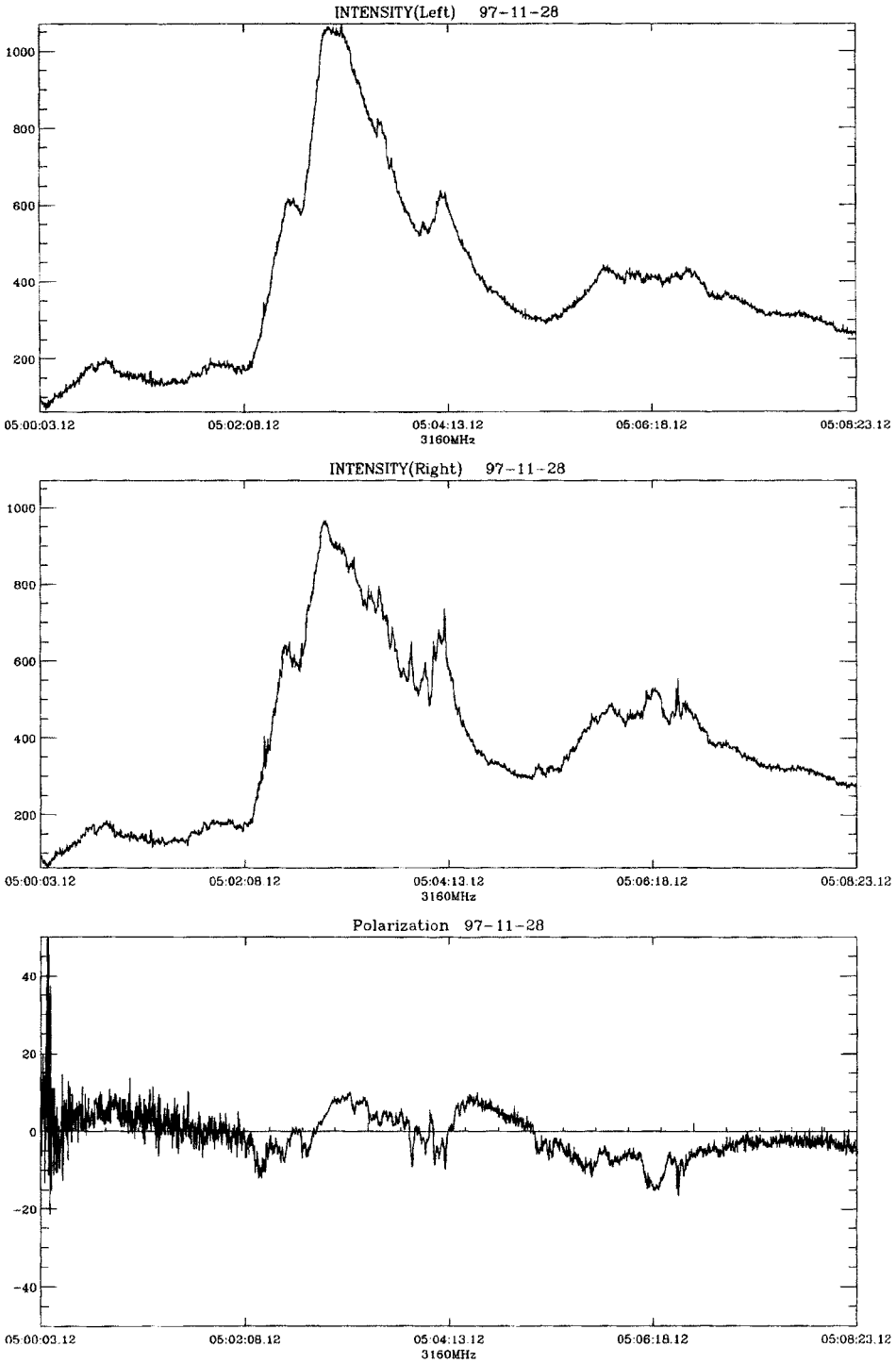
INTENSITY(Left) 97-11-28
1000
800
600
400
200
05:00:03.12
05:02:08.12
05:04:13.12
05:06:18.12
05:08:23.12
3160MHz
INTENSITY(Right) 97-11-28
1000
800
600
400
200
05:00:03.12
05:02:08.12
05:04:13.12
05:06:18.12
05:08:23.12
3160MHz
Polarization 97-11-28
40
20
0
-20
-40
05:00:03.12
05:02:08.12
05:04:13.12
05:06:18.12
05:08:23.12
3160MHz

Figure 2b.

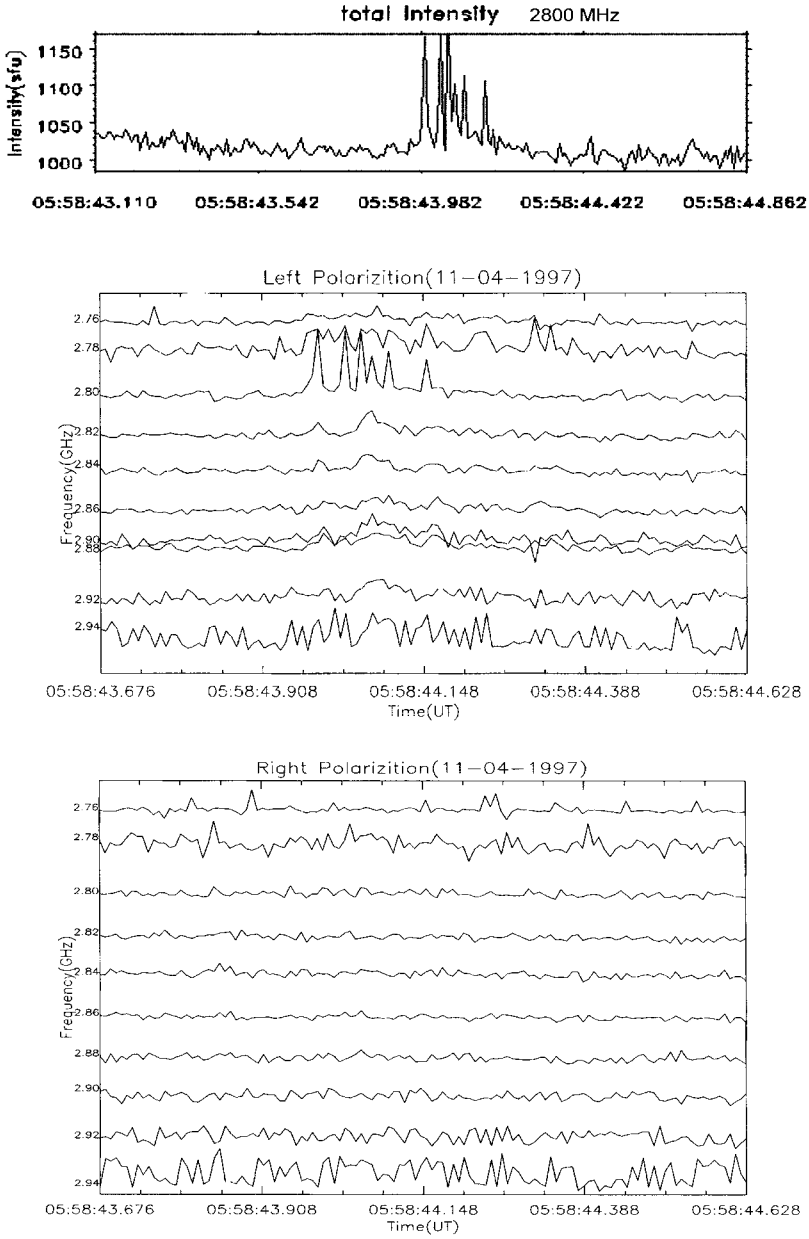

Figure 3a.

Figure 3. Millisecond spikes with high time resolution in two events on 4 and 28 November 1997 as they were seen by microwave spectrograph between 2.6–3.8 GHz at Beijing Astronomical Observatory. (a) 4 November event. *Top*: radio profiles in total intensity in SFU. *Center*: multichannel presentation of the same group of spikes visible only in one LCP channel at 2800 MHz. *Bottom*: RCP channels at the same frequencies. (b) 28 November event. One-channel presentation at 3160 MHz in arbitrary units of numerous spikes, visible only in RCP channels (*middle*). *Bottom*: dynamic spectrum between 2.95–3.41 MHz. The duration of each isolated spike is at the limit of the instrument time resolution (one pixel $\approx$ 8 ms).

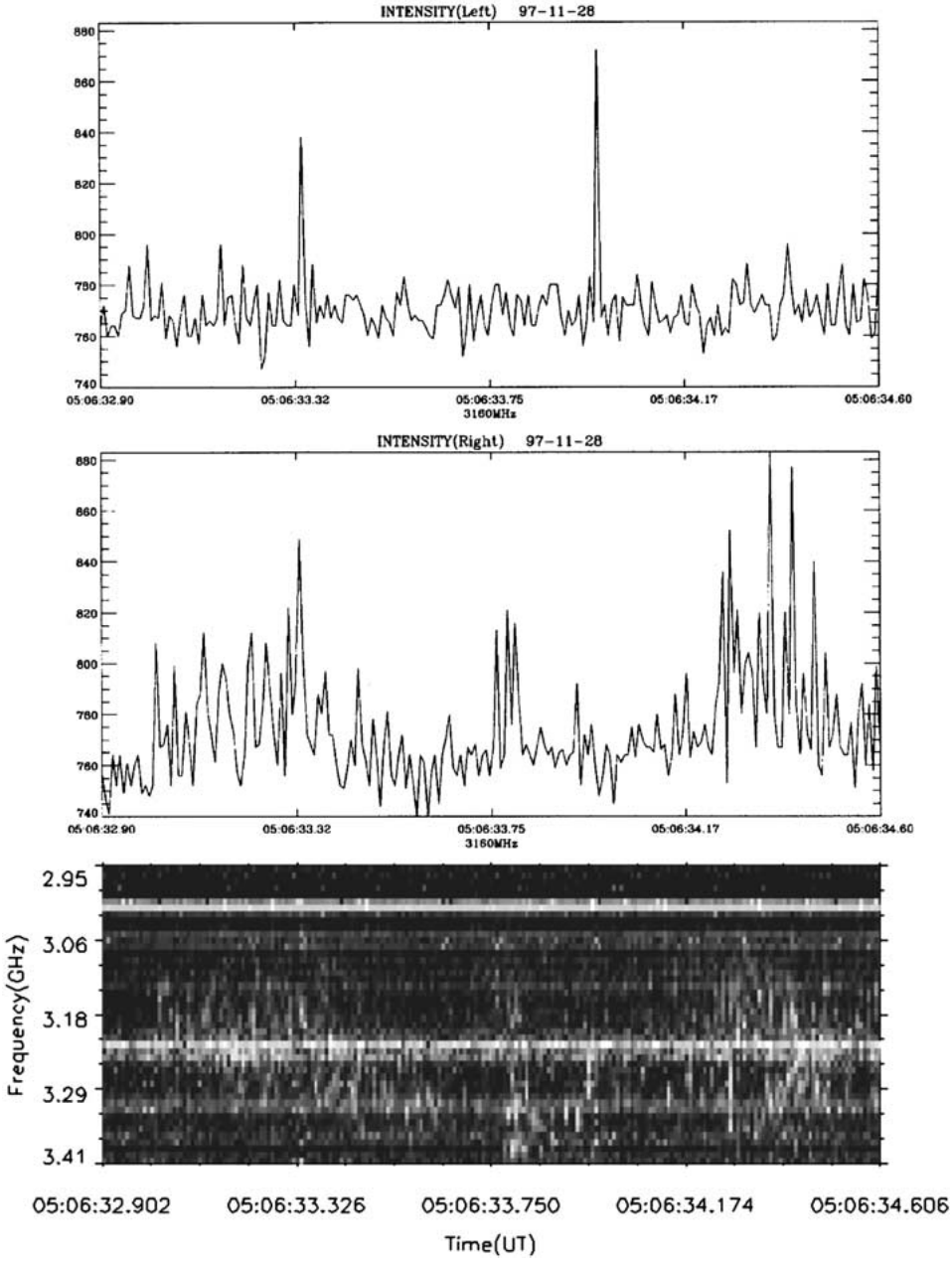
INTENSITY(Left) 97-11-28
880
860
840
820
800
780
760
740
05:06:32.90
05:06:33.32
05:06:33.75
05:06:34.17
05:06:34.60
3160MHz
INTENSITY(Right) 97-11-28
880
860
840
820
800
780
760
740
05:06:32.90
05:06:33.32
05:06:33.75
05:06:34.17
05:06:34.60
3160MHz
Frequency(GHz)
2.95
3.06
3.18
3.29
3.41
05:06:32.902
05:06:33.326
05:06:33.750
05:06:34.174
05:06:34.606
Time(UT)

Figure 3b.

TABLE I
Parameters of ms spikes in five events

Date	UT	Half-power duration (ms)	Flux (s.f.u.)	Hα flare	Polari-zation	Magn. polarity	Wave mode
14 May 1993	23:08	20	160	N20 E48	R 20	N	X
25 November 1996	05:13	20	20	S08 W15	0	S	-
4 November 1997	05:58	10	145	S13 W33	L 80	S	X
28 November 1997	05:00	10	10	N18 W70	R 100	N	X
15 April 1998	08:00	10	10	N29 W15	R 100	N	X

and 28 November 1997 a wave mode was defined using the magnetic polarity of the leader spot in AR, since that was justified by the similar coincidence in other events.

The polarization of emission of both microwave bursts (4 and 28 November 1997, discussed in detail here) was weak during the events and corresponded to *X* mode at the moments of spike emission.

Positions of radio sources above magnetic maps are shown in Figure 4. At the top two parts of SOHO MDI magnetograms are shown nearest to the flare times of 4 November 1997 in AR 8100 (left) and 28 November 1997 in AR 8113 (right). We have the radio positional data only at 5.7 GHz with the Siberian Solar Radio Telescope, and in the bottom we can see their positions overlain on respective MDI magnetograms. At the bottom of Figure 4 one can see double radio sources above the leader and trailing spots, but both radio bursts developed in the right sources. Both flares appeared also above the leader spots, therefore we believe that spike sources had taken place also above the leader spots in both events. The magnetograms show closest opposite magnetic polarities above the leader spots (essentially in AR 8113), and in this connection the X-magnetoionic mode, defined above for spike emission using the polarity of leader spots was uncertain.

2.1.2. *Some Conclusions from Radio Data*

Millisecond spikes under discussion are a peculiar type of very fast spikes (in comparison with microwave spikes discussed in the literature) at the limit of time and frequency resolution: duration ≤ 8 ms, frequency bandwidth $\leq 10-20$ MHz.

The sign of circular polarization corresponds to the extraordinary mode (on the polarity of the leader spot), although taking into account a multipolarity in the radio sources as was shown for the events of 4 and 28 November 1997, such a conclusion is not certain, and must admit a possibility of the mode conversion during propagation, essentially to explain a weak polarization degree, as is sometimes observed.

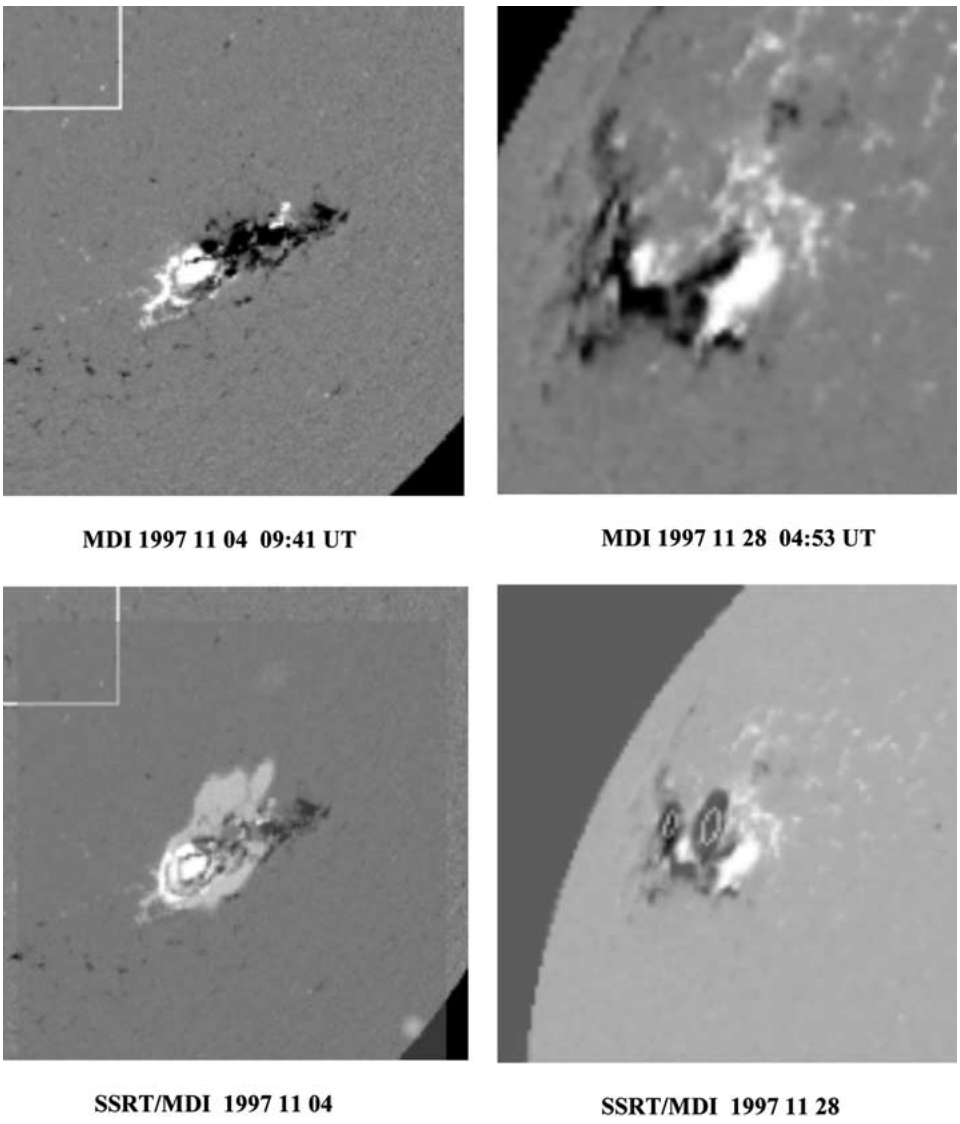

Figure 4. SOHO/MDI magnetograms of AR 8100 after the flare 4 November (*top left*), and AR 8113 just before the flare 28 November (*top right*). *Below*: positions of the respective double radio sources at 5.7 GHz from the Siberian Solar Radio Telescope (contours at a half intensity level, courtesy of A. Altyntsev and V. Zandanov) overlapped on MDI magnetograms. Burst sources localized at the right sources in both events, above the leader spots.

Spikes are usually recorded just after the intensity maximum of microwave bursts, and the intensity flux of spikes in 5 events was about 10% of the total of the microwave bursts.

We do not have any exact positional data of spike sources, and we could only propose very small source dimensions for such very fast spikes and therefore very high brightness temperature.

2.1.3. *Optical and SOHO/EIT Data*

The evolution of the 4 and 28 November flares is shown in Figures 5 and 6. Figure 5 presents the beginning of the flare in Hα (6563 Å) from Learmonth station and Hβ (4861 Å) from Huairou station (BAO). The flare happened above the leading spot of the active region with south polarity according to the magnetograms of KPNO, SOHO/MDI and Huairou station for this day. Therefore the spike emission corresponds to the extraordinary magnetoionic mode. The Hα flare shows a helmet structure high above the leader spot. Similar structures with a bright loop top can be seen in the Hβ picture, with the white line at the top left of the figure having a scale 30 arc sec.

SOHO/EIT movie images in the Fe XII 195 Å line (displaying hot loops with $T_e \approx 2 \times 10^6$ K) show similar forms of hot flare areas above the leader spot and ejections to the north above the helmet structure visible in Hα (see the four frames in Figure 6 from full-disk SOHO/EIT movie images). Figures 5 and 6 suggest a magnetic reconnection with an X-point just above the helmet structure in Hα, and EIT images indicate a fast downflow and an upward ejection (CME). A big loop with scale $\approx$ 60 000 km between leader and trailing spots visible in all UV and *Yohkoh*/SXT images was stable during the event.

LASCO C2 and C3 images show a halo CME at 06:10 UT and we associated the escape of the CME just above the leading spot with ejections in EIT 195 images after this moment.

Two frames of the 28 November flare in EIT 195 Å and 284 Å lines are shown at the bottom of Figure 6. The left image in the EIT 195 Å line displays some bright flare kernels in different loop legs just before the flare. The right image in the EIT Fe XV 284 Å line shows some hot post-flare magnetic loops as an arcade with 5 loops with $T_e \approx 2.6 \times 10^6$ K. Consecutive brightenings of different flare kernels in different loops explains repeated polarization reversals during the event shown in Figure 2(b). Therefore, one needs a very careful estimation of magnetic polarity under each increase of radio emission, and radio magnetoionic modes in the last column of Table I are not certain because one can see in the magnetograms (the top of Figure 4) some very close kernels with opposite magnetic polarities.

2.1.4. *Yohkoh/SXT and HXT Data (T_e and EM Maps)*

In *Yohkoh*/SXT images in the open ALMg filter (top of Figure 7) one can see a bright emission area above the trailing spot at the beginning of the 4 November event (05:52 UT) and a strong emission (in saturation) above the leader spot at the

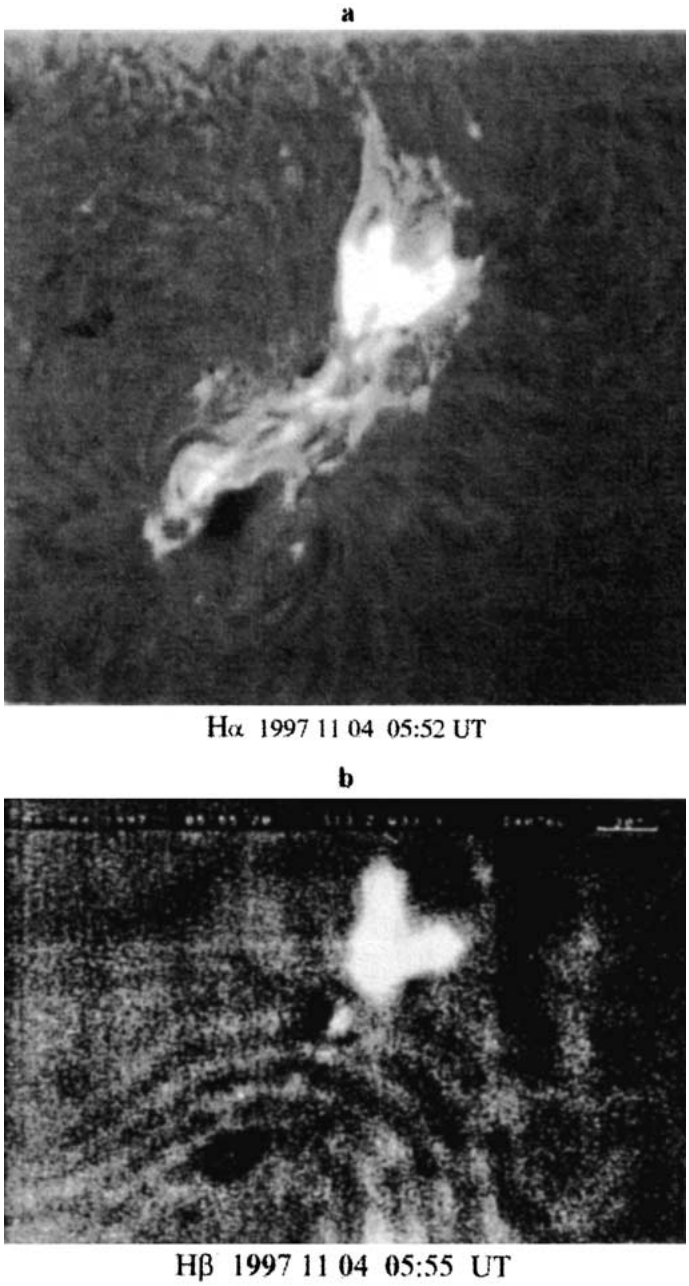

Figure 5. The beginning of flare in NOAA AR 8100 in the event 4 November 1997 in Hα (Learmonth station) (a) and Hβ (b) lines (Huairou station of BAO). The flare took place above the leader spot of AR of south polarity according to the SOHO/MDI magnetograms (magnetograms of KPNO, Holloman AFB (New Mexico) and Huairou station (BAO) for this day were also used). The Hα flare shows a helmet structure high above the leader spot. Similar structures with a bright loop top can be seen in the Hβ picture. The bar at the top right of the Hβ image shows the scale of 30 arc sec.

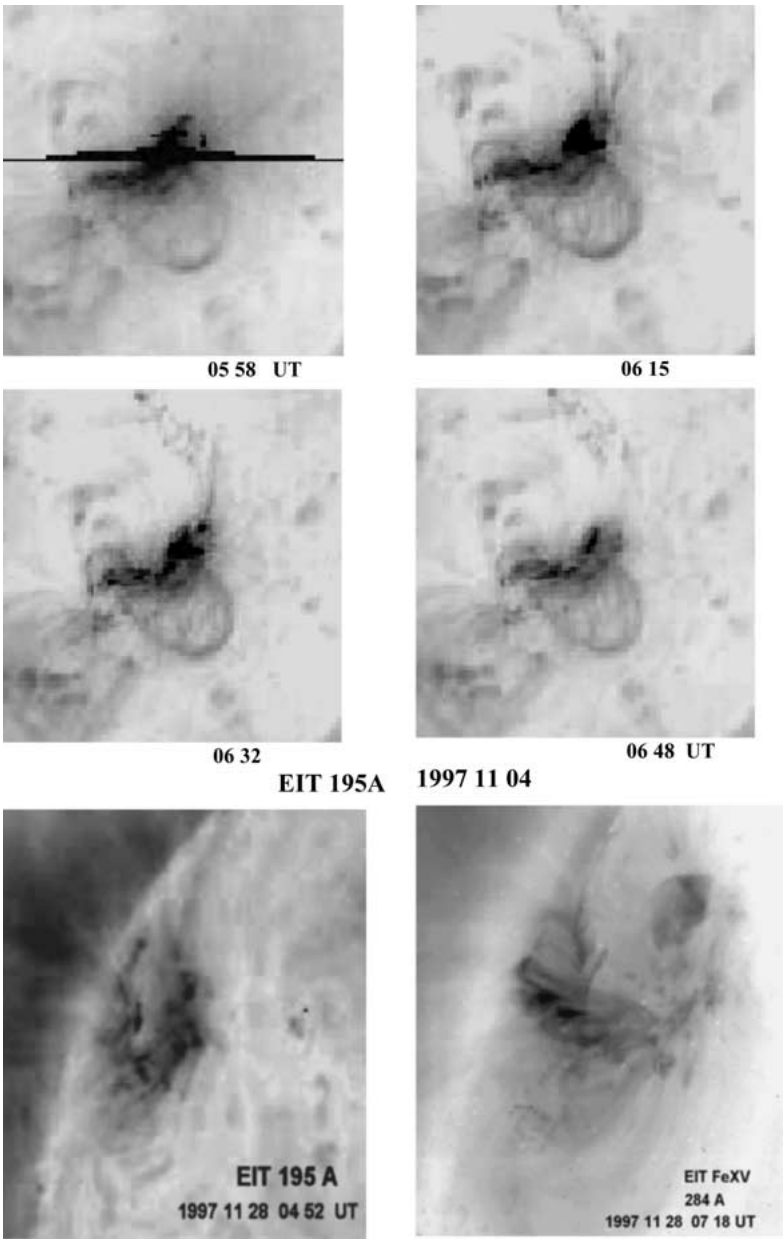

Figure 6. Four frames from full-disk SOHO/EIT movie images at 195 Å (4 November event) show a hot area with $T_e \approx 2 \times 10^6$ K in the descending phase of the flare and ejections in the same place just above the helmet structure in Hα coinciding in time with the CME seen by LASCO C2. The first frame shows the maximum phase of flare near 05:58 UT. *At the bottom*: two frames from SOHO/EIT for the 28 November flare (AR 8113 at the east limb). The left frame in EIT 195 Å shows the beginning of flare at 04:52 UT as numerous hot flare kernels. The right one from EIT 284 Å displays post flare loops. Consecutive brightenings of different flare kernels explains repeated polarization reversals during the event shown in Figure 2(b).

burst maximum in accordance with the polarization change at microwaves in the beginning (Figure 2(a)) and with the helmet structure visible at Hα and Hβ pictures (Figure 5).

In the middle of Figure 7 the flare is seen in SXT Al12 and Be119 filters at 06:10:32 UT from calibrated data with the field of view displaced in the north-west direction. The scale of the field view is about 114 073 km with one pixel 2.46×2.46 arc sec.

At the bottom of Figure 7 the temperature and volume emission measure (EM) maps are shown using the ratio of the Be119/Al12 filters for the same moment at 06:10:32 UT. The contours in the EM map correspond to values 125, 500, 2000×10^{44} cm^{-3} for one pixel, and the thick contour shows the value 500. The value of EM is a total EM in a $2.46'' \times 2.46''$ pixel. The EM maps and soft X-ray images are displayed in log-scale. The temperature scale of pixels includes values 8, 10, 12, 14, 16, and 18 MK, and the thick contour shows $T_e = 10$ MK. In bright (black) points at the center of the flare area $T_e = 18$ MK. Similar values of T_e exist in numerous bright points around of the flare area, probably along the reconnecting magnetic loops.

The evolution of the 28 November event using SXT temperature and EM maps for three moments just after the flare maximum is shown in Figure 8. The contours of the temperature maps show 10 MK (thick line), 15 MK, and 20 MK. Those on the EM maps show 10^{47}, 10^{48} (thick line), and 10^{49} cm^{-3} for one pixel. We can see an ejection in the north direction as a consequence of the magnetic reconnection.

On 4 November, at the moment 06:10 UT one can see a remnant of the AR after the burst maximum. Nevertheless, the hottest source with $T_e \geq 18$ MK as a narrow line in the horizontal direction in the center of SXR source might be a manifestation of a narrow fast shock front propagating downward from an X-reconnection point as was proposed and observed by Tsuneta (1996).

However the maximum of EM (as the densest emission volume in SXR) is elongated in the vertical direction, close to a helmet form (see left bottom in Figure 7). The diameter of the loop (FWHM value) is about 13 660 km. Then for a maximal EM value 2000×10^{44} cm^{-3} for one pixel ($2.46'' \times 2.46''$) according to the averaged formula $EM \approx n_e^2 q d$ (with a filling factor $q \approx 1$) in Krucker *et al.* (1995b), we have the electron density in a hot bright SXR center $n_e \approx 6.32 \times 10^{10}$ cm^{-3}, i.e., a plasma frequency $f_p \approx 2270$ MHz (close to observed frequency band of spikes).

Moreover, we see a hot contour (composed from numerous bright points) around the whole SXR source as high T ridges along magnetic loops (similar to pictures by Tsuneta, 1996). In those magnetic loops the plasma is more rarefied: a similar estimation of n_e for $EM \approx 125 \times 10^{44}$ cm^{-3} for one pixel and a loop diameter $d \approx 2000$ km gives $n_e = 4 \times 10^{10}$ cm^{-3}.

The same picture for the event of 28 November 1997 at the moment of spikes also demonstrates high T ridges along reconnecting magnetic loops and in the upper part they have a cross-piece as a possible fast shock front (see Figure 8 just at the spike moment 05:06:50 UT). An estimation of n_e at the center of the flare

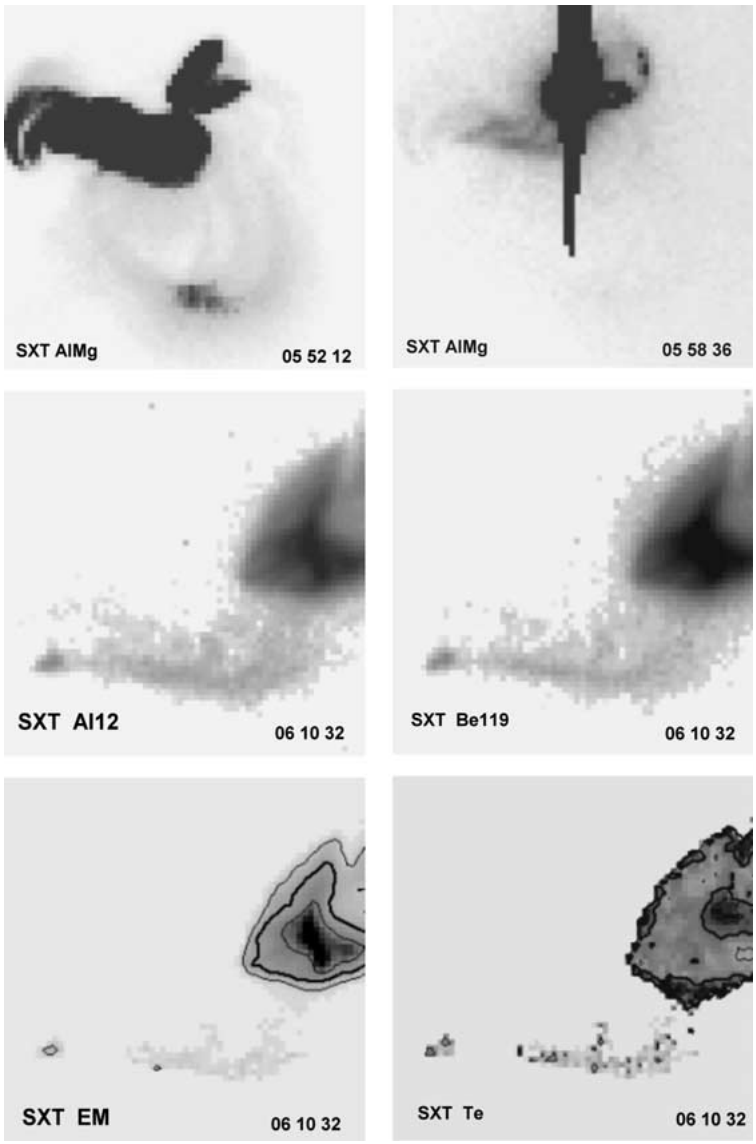

Figure 7. Yohkoh/SXT images in AR 8100 for the event of 4 November 1997. In the *top left* image (with open/AlMg filter) we can see a bright emission area above the trailing spot at the beginning of the event (05:52:12 UT). The *top right* image (with NuDen/AlMg filter) shows strong emission (in saturation) above the leading spot at the burst maximum (05:58:36 UT), in accordance with helmet structure visible at Hα and Hβ pictures and with the polarization change at microwaves at the beginning of the event (Figure 2(a)). *At the center*: two frames of calibrated data in Al12 and Be119 filters after the flare maximum 06:10:32 UT. The *bottom left* image shows the emission measure map at the same time; the *thick line* corresponds to 500×10^{44} cm^{-3}. *Bottom right*: the temperature map from the ratio Be119/Al12 filters at 06:10:32 UT; the *thick contour* shows $T_e = 10$ MK. The images are 64×64 pixels and one pixel is 2.46×2.46 arc sec. A narrow horizontal hot (*black*) line (three pixels at the center of the flare area just above an almost vertical region with the maximum *EM* (*bottom left*)) with $T_e \approx 18$ MK shows the probable position of a fast shock front.

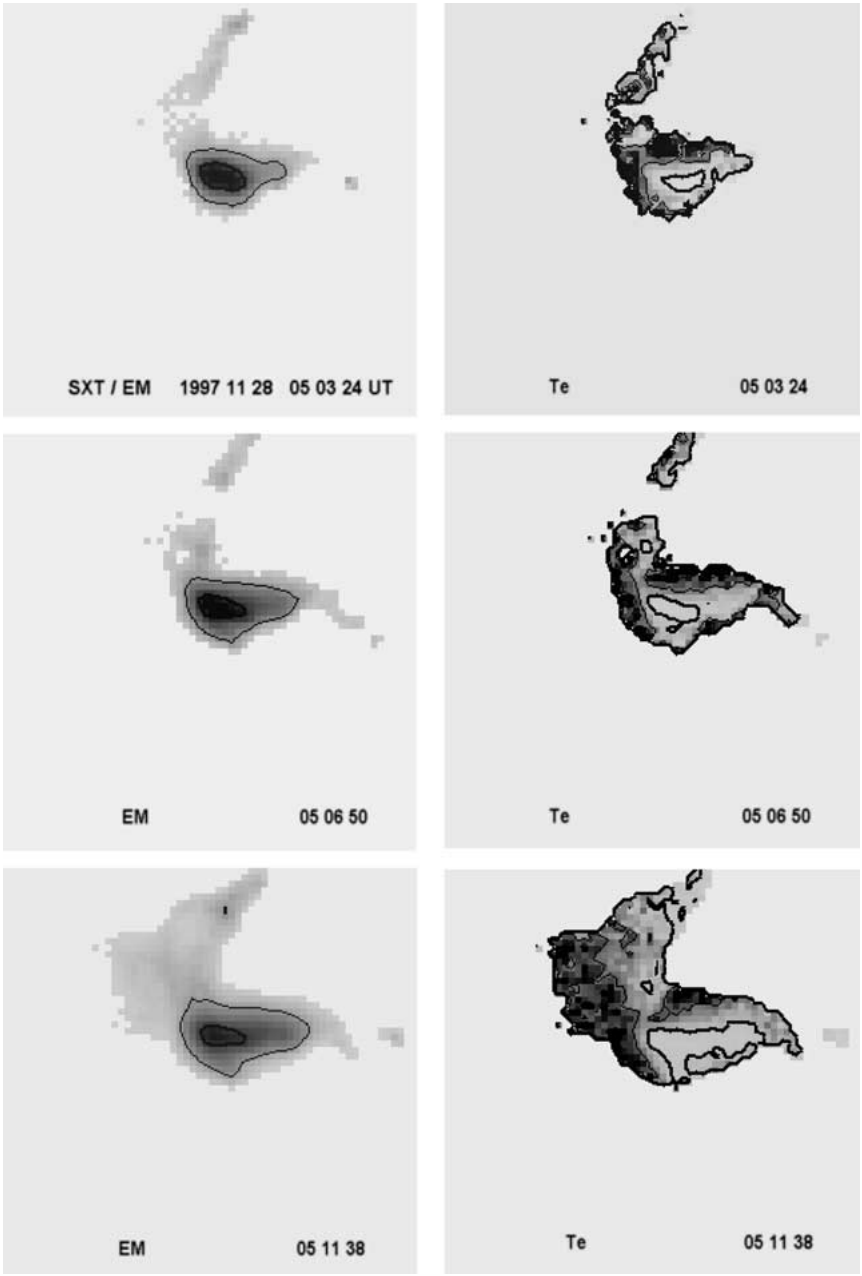

Figure 8. The evolution of the 28 November event (AR 8113) using *Yohkoh*/SXT temperature maps and volume emission measure maps for three moments after the flare maximum. The temperature maps are calculated from the ratio Be119/Al12 filters, the *thick contour* shows $T_e = 10$ MK and the brightest points (*black*) are $T_e = 20$ MK. Unlike the 4 November event this flare was located very near to the east limb and the probable position of the fast perpendicular shock front is visible as a cross-piece between two hot loops with $T_e \approx 20$ MK above the EM maximum. In the emission measure maps the *thick line* corresponds to $EM = 10^{48}$ cm^{-3} and in the center 10^{49} cm^{-3} for one pixel.

region with $EM \approx 10^{49}$ gives here $n_e \approx 1.3 \times 10^{12}$ cm^{-3}. And the hot magnetic loops are also more rarefied: $n_e \approx 1.3 \times 10^{11}$ cm^{-3}. Higher densities for this flare suggest that a larger quantity of the evaporated photosphere mass exists at lower heights (in comparison with the 4 November flare). We believe that the locations of the spike radio source are near the mentioned cross-piece where $EM \approx 10^{47}$, i.e, $N_e \approx 10^{11}$ cm^{-3} and $f_p \approx 3000$ MHz (close to observed frequencies of spikes).

In addition to the 28 November event we analysed the evolution of the HXR emission. In Figure 9 *Yohkoh*/HXT contours are shown for two moments near the flare maximum in the band M2 and near the spike emission in the L band overlapped on SXT images in Be119 and Al12 filters, respectively. The image scale is 64 pixels corresponding to 114 073 km. In the more energetic bands M2 and H one can see a clearly double source in HXR (probably as footpoints of the loop) during the event, but in the low-energy L band we see only one source at the top of the same loop just between the double sources in the M2 band at the peak moment. It coincides with the SXR maximum.

One can see the evolution of HXR sources in the L band: an additional small source appeared just after the flare maximum at the same moments of spike emission at 05:06 UT (in the lower part of Figure 9). This additional maximum is visible also in the M1 energy band.

According to Tsuneta (1996) the hard X-ray source above the loop top may be a main sign of fast perpendicular shock heating. One can see at the moment of spike emission an additional HXR maximum in the L band coinciding with the above mentioned cross-piece in the T_e map (see Figure 8). About 70–80% of the L band counts originate in the thermal plasma. So, basically, the map using the L band shows the thermal plasma. The temperature in these HXR sources may be 30–35 MK.

3. Source Model

Our complete optical and X-ray data for the 4 and 28 November events provide evidence of magnetic reconnection and the presence of fast shock fronts in the flare region just at the moment of spike emission. The spike emission differs considerably from the emission of entire microwave bursts. Since spikes are very fast and narrow band pulses of radio emission with a high degree of circular polarization, they appear only episodically after the flare maximum. Therefore, the spike emission might have rather another nature and may be connected with fast shock fronts, propagating from the X-point of a magnetic reconnection, when the energetic condition for a fast shock holds near the loop top, namely when Mach number $M = V/C_s$ exceeds 1. Here V is the downstream plasma velocity from the X-point and C_s is the sound velocity (Tsuneta, 1996).

Spatial and time coincidences of HXR and microwave sources connect the same fast particles responsible for those emissions and a common acceleration source

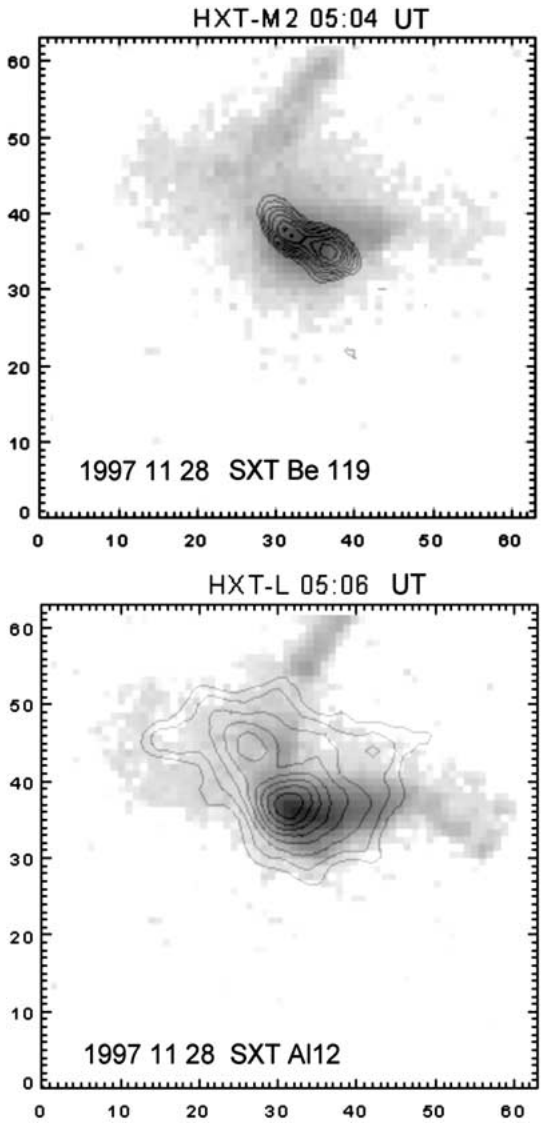

Figure 9. Yohkoh/HXT contours for two moments of the 28 November event near flare maximum in the M2 band, and near the moment of the spike emission in the L band overlapped on SXT images in Be119 and Al12 filters respectively. The image range of 64 pixels is about 114 073 km. If in the more energetic M2 band we see the double HXR source as footpoints of a small flare loop, then in the L band the main maximum takes place just between the two sources in the M2 band, i.e., at the loop top and coincident with the SXR maximum. According to Tsuneta (1996) the hard X-ray source above the loop top may be a main signature of fast perpendicular shock heating. One can see at the moment of spikes (05:06 UT) an additional HXR maximum, coinciding with the mentioned cross-piece in the T_e map. The temperature in these HXR sources may be 30–35 MK.

which is usually proposed as connected with magnetic reconnection at middle heights in the corona ($\geq$ 10 000 km).

According to accepted ideas about spike sources they are also connected with a reconnection region and particles accelerated in such a region can propagate upward and cause meter radio bursts and downward to cause successively decimetric, microwave and HXR emissions. A similar scheme was proposed for spikes by Fu *et al.* (1990) at $\lambda = 21$ cm.

We propose that after the escape of a CME, during the restoration of the magnetic structure, a reconnection region with an X-point remained during the burst and here we emphasize the fact that from the X-point two fast shocks (upward and downward) and two pairs of slow shocks along magnetic lines must move away from the X-point. A similar model was used in Chernov (1990) for the fine structure of type IV bursts, and it was confirmed by a set of new simulations (Yokoyama and Shibata, 1996) and observations (Tsuneta, 1996).

According to well-accepted ideas shock fronts are the place of Langmuir, ion-sound and whistler instabilities. All these waves are usually observed *in situ* in interplanetary shocks and in the front of the Earth bow shock (Gurnett *et al.*, 1979).

So, any model of spike emission must take into account that the radio source is usually located in a region of magnetic reconnection, but not for one isolated spike. This is a sufficiently extended region as the source of fast particles responsible for the whole microwave burst. Microwave emission must be generated below (before the fast shock front) by fast particles at some cyclotron harmonics (Zheleznyakov, 1970).

Langmuir waves just around the reconnection region can contribute to the emission of decimetric bursts. In most events we observe some maxima only in the decimetric range. The plasma density in the shock front must be 2–3 times higher relative to the ambient plasma density, therefore the plasma frequency in the shock front may be about the same as in the lower-lying microwave source.

According to our conclusion from the observations, a mechanism of spike emission must operate in direct association with shock fronts, where Langmuir and ion-sound waves instabilities are developed. Therefore the most probable mechanism of spike emission may be the interaction of plasma Langmuir waves with ion-sound waves $l + s \rightarrow t$. This process is well studied and directly connected with radio type I bursts by Benz and Wentzel (1981).

4. Wave–Wave Interaction $l + s \Rightarrow t$

We need to explain short-lasting emission of isolated spikes (from 0.1 s in the meter range up to some ms at microwave) with $T_b \geq 10^{13}-10^{15}$ K from probably a small source, but of unknown size. The preferential magnetoionic mode is the ordinary one with a possibility to convert (partially) into an extraordinary mode.

The preferential extraordinary mode reported by Güdel and Zlobec (1991) for decimetric spikes may be due to confusion with the magnetic field polarity since small spike sources may be located far enough from type III sources in the opposite magnetic field direction.

According to our conclusion from the observations, a mechanism for spike emission must operate in direct connection with shock fronts where Langmuir and ion-sound wave instabilities develop. Therefore the most probable mechanism of spike emission may be the interaction of plasma Langmuir waves with ion-sound waves. This process is well studied by Tsytovich (1971), Melrose (1980) and in direct connection with radio type I bursts by Benz and Wentzel (1981). In the last paper it is proposed that ion-sound waves may be generated in a current sheet in the region of a small magnetic reconnection. Later a small magnetic reconnection with fragmentary energy release was implied for a single spike emission (Benz, 1986).

As Benz and Wentzel proposed, ion-sound waves are generated by current driven instability. The waves generate an anomalous resistance and create the conditions for their existence with $T_e \gg T_i$. However, Melrose (1989) believes that the mechanism by which these waves are generated is not understood and there is no basis for expecting them to be present in the corona other than by analogy with the interplanetary medium (Gurnett *et al.*, 1979). In such a case ion-sound waves could be present only in the narrow shock fronts. At the same time all the energetic estimations of Benz and Wentzel (1981) for the coalescence $l + s \rightarrow t$ remain available for our consideration here. However, the three-wave matching conditions were not strictly verified.

4.1. Testing of the conservation laws

To be certain of the resonance coupling of l and s waves in the solar corona we must verify the matching conditions of frequency and wave vector at the sum frequency $l + s \rightarrow t$ and at the difference frequency $l \rightarrow t + s$ (the decay process):

$$\omega_l \pm \omega_s = \omega_t, \qquad k_l \pm k_s = k_t \ , \tag{1}$$

to determine the ranges of possible angles between the wave vectors of all resonance modes and magnetic field directions **B** $(\theta_l, \theta_s, \theta_t)$.

Therefore we use simple dispersion relations for all modes but with allowance for the magnetic field:

$$\omega_l^2 = \omega_{\mathrm{Pe}}^2 + 3k_l^2 V_{\mathrm{Te}}^2 + \omega_{\mathrm{Be}}^2 \sin^2 \theta_l \ , \tag{2}$$

$$\omega_t^2 = k_t^2 c^2 + \omega_{\mathrm{Pe}}^2 \left(1 + \frac{\omega_{\mathrm{Be}}}{\omega_t} \cos \theta_t\right)^{-1} \ , \tag{3}$$

$$\omega_s^2 = k_s^2 v_s^2 \ . \tag{3}$$

It is evident from the dispersion curves that only an ordinary wave can participate in such an interaction, at least for the usual wave numbers k_l and $k_s \geq \omega_{\mathrm{Pe}}/c$ which are the most probable when the emission source is located between the escape levels of ordinary and extraordinary waves, although according to Tsytovich (1970) in the whole range of k_s, i.e., $\omega_{Pi}/v_s < k_s < \omega_{\mathrm{Pe}}/V_{T_e}$ ion-sound waves can interact with Langmuir waves.

We simplify the first two equations using expansions subject to the condition that their second and third terms are small and $\omega_{\mathrm{Pe}}/\omega_{\mathrm{Be}} \gg 1$:

$$\omega_l \approx \omega_{\mathrm{Pe}} \left(1 + \frac{3k_l^2 V_{Te}^2}{2\omega_{\mathrm{Pe}}^2} + \frac{\omega_{\mathrm{Be}}^2 \sin^2 \theta_l}{2\omega_{\mathrm{Pe}}^2}\right) , \tag{5}$$

$$\omega_t \approx \omega_{\mathrm{Pe}} \left(1 + \frac{k_t^2 c^2}{2\omega_{\mathrm{Pe}}^2} - \frac{\omega_{\mathrm{Be}}}{2\omega_{\mathrm{Pe}}} \cos \theta_l\right) . \tag{6}$$

We substitute these expansions in the first resonance condition (1) $\omega_l \pm \omega_s = \omega_t$, then determine k_t^2 from the result, and substitute it in the relation for wave numbers:

$$k_t^2 = k_l^2 + k_s^2 \pm 2k_l k_s \cos\theta , \tag{7}$$

where θ is the angle between the vectors $\mathbf{k}_l$ and $\mathbf{k}_s$. We obtain:

$$k_t^2 = \frac{1}{c^2}(\omega_{\mathrm{Pe}}\omega_{\mathrm{Be}} \cos\theta_t + \omega_{\mathrm{Be}}^2 \sin^2 \theta_l + 3k_l^2 V_{\mathrm{Te}}^2 + 2k_s v_s) . \tag{8}$$

Using the procedure to eliminate k_t we estimate cos θ_t:

$$\cos \theta_t = \frac{k_s^2 c^2}{\omega_{\mathrm{Pe}}\omega_{\mathrm{Be}}} \left[\frac{k_l^2}{k_s^2}\left(1 - 3\frac{V_{Te}^2}{c^2}\right) \mp 2\frac{k_l}{k_s}\cos\theta + 1\right] - \frac{\omega_{\mathrm{Be}}}{\omega_{\mathrm{Pe}}} \sin^2 \theta_l \pm 2\frac{k_s v_s}{\omega_{\mathrm{Be}}} . \tag{9}$$

Here the ratio k_l/k_s is used as a convenient parameter. It is easy to verify that for small values of θ_l and θ, justified by the evident fact that the coalescence $l + s \to t$ and the decay $l \to t + s$ take place respectively with almost antiparallel or parallel wave vectors $\mathbf{k}_l$ and $\mathbf{k}_s$ (an analogy exists with the similar processes of Langmuir waves and whistlers (Fomichev and Fainstein, 1988; Chernov and Fomichev, 1989)) and for a small magnitude of the ratio $\omega_{\mathrm{Be}}/\omega_{\mathrm{Pe}} \sim 0.1$, the quantity cos θ_t is determined mainly by the last term in (9). Taking into account that the lower sign corresponds to the process at the sum frequency $l + s \to t$ with $k_l \approx -k_s$ and the upper sign to the process at the difference frequency $l \to t + s$ with $k_l \approx k_s$ and that $k_s v_s = \omega_s$, we can write:

$$\theta_t \approx \mp \text{ arc } \cos 2\frac{\omega_s}{\omega_{\mathrm{Be}}} . \tag{10}$$

The angle θ_t is somewhat larger or smaller than this value, depending on the sign of the bracketed term in (9); the sign, in turn, is governed mainly by the ratio k_l/k_s, which is very close to unity, i.e., k_t is directed in the side of the biggest from k_l, k_s.

The bracketed term in (9) changes sign when

$$\left(\frac{k_l}{k_s}\right)^2 \left(1 - 3\frac{V_{Te}^2}{c^2}\right) - 2\left(\frac{k_l}{k_s}\right) \cos\theta + 1 = 0\,. \tag{11}$$

In such a case

$$\frac{k_l}{k_s} = \frac{\pm\cos\theta \pm \sqrt{\cos^2\theta - (1 - 3V_{Te}^2/c^2)}}{1 - 3V_{Te}^2/c^2}\,. \tag{12}$$

In order for k_l/k_s to be real-valued, it is necessary that $\cos^2\theta - (1{-}3\ V_{Te}^2/c^2) > 0$, i.e., $\cos\theta > \pm\sqrt{1 - 3V_{Te}^2/c^2}$, so the upper bound of the angle $\theta < 1.28°$ is obtained at the coronal temperature $T_e = 10^6$ K, or for $V_{Te} \approx 3.89 \times 10^8$ cm s^{-1}, and $\theta < 8.14°$ for $T_e = 2 \times 10^7$ K. We then obtain from (12) the two values $k_l/k_s = 1.00235$ and 0.99816, i.e., the bracketed term in (9) changes sign when the ratio k_l/k_s passes through unity.

The evident condition $|\cos\theta| < 1$ leads to the limitation of k_s from above: $k_s < 0.5\omega_{\mathrm{Be}/v_s}$. This value is about two times bigger than the Debye length $k_D = \omega_{\mathrm{Pe}}/V_{Te}$, therefore the interaction is possible in the whole range of k_s and $k_l \approx k_s$.

The range of θ_t for a simple rough estimation from (10) will determined by the frequency range of s-waves: $\omega_{Bi} < \omega_s < \omega_{Pi}$. Substituting these limiting frequencies in (10), we obtain that the decay at the difference frequency yields the emission of t-waves in the range of angles $62° < \theta_t < 89°$ and, respectively, for the coalescence at the sum frequency $91° < \theta_t < 118°$.

4.2. Brightness temperature and radiation process

4.2.1. *Brightness Temperature*

Now it is clear that the ls-interaction is very similar to the interaction of plasma waves with whistlers (Fomichev and Fainstein, 1988; Chernov and Fomichev, 1989). Only in the last process the whistler's wave numbers have a considerable limitation (from below and from above). Otherwise these two interactions are equally efficient. According to Benz and Wentzel (1981) ls-interaction becomes the most efficient with a high intensity of s waves, when unit optical thickness is reached over merely a few meters.

It is easy to show that in an optically thick source the interactions at the frequencies $\omega_t = \omega_l \pm \omega_s$ can be equally efficient and the maximum brightness temperature can be derived (similar to the procedure in Benz and Wentzel (1981) and in Chernov and Fomichev (1989)):

$$T_b = \frac{h\omega_{\mathrm{Pe}}}{k_B}\frac{N_s N_l}{N_s \pm N_l}\,, \tag{13}$$

where h is Planck's constant, k_B is Boltzmann's constant, and N_l, N_s are the dimensionless wave intensities ($N_l \ll N_s$) (or wave quantum densities). That is the theoretical estimation. From the observation we obtain

$$T_b = \frac{2\pi^2}{k_B}\frac{W_t}{k_t^2 \Delta k_t} = \frac{0.143 \times 10^7 S(\text{s.f.u.})}{f^2 l_{10}^2} \exp^{\tau} \ , \tag{14}$$

where τ is the optical depth of the solar corona for the electromagnetic emission.

The designations are similar to Fomichev and Fainstein (1988): S(s.f.u.) is the burst flux in solar flux units, f is the frequency in GHz, and l_{10} is the linear source size perpendicular to the line of sight in units of 10^{10} cm. So that with a flux emission 100 s.f.u. and a burst source of 10^8 cm we obtain the observed $T_b \approx 7 \times 10^{13}$ K, i.e., close to the value predicted in Benz and Wentzel, for instance, with a small value of density energy of plasma wave $W_l \approx 10^{-7}$ erg cm^{-3} for isotropic l-waves, and $W_l = (h/(2\pi)^3)\omega_{\text{Pe}} N_l k_l^2 \Delta k_l \Omega_l$. So with a solid angle $\Omega_l \leq 1$, $k_l \approx \Delta k_l \approx 5 \times 10^{-2}$ cm^{-1} we find from (13) for $N_l \ll N_s$, $T_b \approx 5.7 \times 10^{13}$ K.

4.2.2. *Burst Parameters*

The duration of an individual spike may be determined by the particle acceleration mechanism. According to the modelling of explosive reconnection (after which CMEs escape) of Sakai and Ohsava (1987) the quasiperiodic acceleration of ions and electrons up to high energy by the induced electric field takes place with a period $\approx 10\ \omega_{Bi} \approx 10^{-5}$–$10^{-6}$ s. So that, first of all, such particles generate ms spikes of Langmuir waves. In interplanetary shocks such spikes of Langmuir waves were observed (see Gurnett *et al.*, 1979). The energy level of ion-sound waves in the shock front may be almost constant for some seconds during which the temperature equalization ($T_e \approx T_i$) takes place. According to Tsytovich (1977) this time depends mainly on the electron-ion collision frequency (ν_{ei}): $\tau_e \approx (m_i/3m_e)\nu_{ei}^{-1}$. For $\nu_{ei} = 100$ we obtain $\tau_e \approx 6$ s. In reality, ms spikes are usually observed in series of a few seconds duration.

The narrow bandwidth of an individual spike ($\leq$ 10–30 MHz in the event of 4 November 1997 and some tens of MHz in other events) may be explained by the narrow (in height) source of s-waves, namely by the bandwidth of a shock front $\sim$ 20 m. In other more intense events s-waves may embrace a larger downstream region of shock front and the source thickness of s-waves can be some hundreds m. The perpendicular size of the source (the bandwidth of the shock front near an X-point) may be much broader $\approx 10^6$ m, which is the value we used to estimate T_b.

The model under discussion helps us to propose a new explanation of the observations of decimetric spikes at harmonics $s = 2$–6 (Güdel, 1990). The relativistic gyrosynchrotron maser emission seems implausible in the decimetric range, where the plasma emission mechanism usually plays a main role. As a detail, conformity of spikes at different harmonics was not observed. We may relate the emission of consecutive frequency bands of spikes with consecutive magnetic islands with X-point configurations along a vertical magnetic current sheet. Frequency bandwidths at each harmonic show the vertical size of a zone between two fast shock fronts propagating from one X-point, and the frequency separation between the centers

of each spike band (or harmonic frequency) is defined by the size of magnetic islands between X-points. Multiple magnetic islands are usually supposed during the restoration of the magnetic structure after the escape of CMEs and were obtained in multiple numerical modelling of magnetic reconnection. In such a scheme the emission of each spike is caused by streaming fast electrons propagating upward and downward along magnetic islands and generating Langmuir waves, and a visible discrepancy between the time of maxima in the intensity profiles testifies to the propagation of fast particles.

4.2.3. *Depolarization and Conversion $O-X$ Modes*

Since the ls-interaction provides the ordinary (O) magnetoionic mode and the observation indicates mainly the extraordinary (X) mode with different polarization degree, we need to explain the depolarization of radio emission during the propagation. Two main depolarization mechanisms are usually considered in the literature:

(1) Due to propagation through the quasi-transverse magnetic field or zero magnetic field in the current sheet (Zheleznyakov, 1977; Zheleznyakov and Zlotnik, 1988).

(2) Due to the scattering of radio emission by low frequency waves (Melrose, 1989).

For the second mechanism Melrose chose the whistler as the most probable low-frequency mode. According to Melrose's theory the scattering of an O-mode into an X-mode may be effective only close to the X-mode cut-off frequency with some small-angle scattering and in a very narrow range of the whistler's wave number $\Delta k_w \approx k_w$. Such whistlers may be generated by streaming electrons (generating also Langmuir waves) but in a strong magnetic field and with low streaming speeds.

Such limitations also decrease the possibility of nonlinear parametric instability, including the interaction of an O-mode with whistlers (Wang and Li, 1991; Wang *et al.*, 1997) even if we admit a possibility of strong turbulence in an intense event. Besides, in this theory the authors consider the interaction of high and low frequency waves with fixed wave phases, while in the solar corona a random phase approximation is rather plausible.

The $O-X$ scattering by ion-sound waves is also possible with about the same limitation. This requires $\omega_s/\omega_{Pi} \approx (\omega_{Be}/\omega_{Pe})^{1/2} V_e/c \approx 0.004$ for $\omega_{Be}/\omega_{Pe} = 0.1$. There does not exist any information on such low frequency s-waves in the solar corona.

Taking the above-mentioned limitation of the second (2) mechanism into account we choose the first one as the most probable. The presence of a perpendicular magnetic field is very probable along the line of sight for a microwave source located under closed magnetic lines as was shown in Figure 7 (source B) in Li, Fu, and Li (1991). In our case we clearly see the positions of fast shock fronts (as the source of spikes) just under the X-type neutral points with the vanishing magnetic field (see Figures 5–8).

The long-lasting discrepancy between the theory and observations (the expected coupling is estimated as weak with a coupling ratio $Q \ll 1$, while the observations show the opposite value of Q: moderate $Q \approx 1$ or big $Q \gg 1$) was resolved in some papers. Melrose and Robinson (1994) explore the mode coupling by numerically integrating the transfer equation for polarized radiation across multiple reversals of magnetic lines in a quasi-transverse (QT) region and obtain the strong mode coupling.

Bastian (1995) proposed to take into account the angular scattering of radio emission in turbulent inhomogeneities inside the QT region which reduces considerably the scale of mode coupling ΔL and consequently increases the coupling ratio $Q = (\Delta L \Delta k)^{-1}$. The mode coupling become moderate and strong in QT region as required by the observations. At the same time for the meter radio sources high in the corona (at the top of magnetic loop for type I bursts and in open magnetic lines for type II and III bursts) a QT region may be at the line of sight only for limb sources.

However, Zheleznyakov and Zlotnik (1988) alleviated some of the mentioned difficulties by supposing that the magnetic field vanishes in one QT region as is possible in a current sheet. Using their theory, Chernov and Zlobec (1994) obtained a satisfactory explanation for a moderate polarization degree of the fine structure in some type IV bursts and showed a possibility for polarization reversal.

For our model we relate spike sources with a current sheet with an X-point configuration of magnetic lines and in such a case the radio emission must propagate through a QT region with vanishing magnetic field in the middle of QT region.

The coefficient of conversion in the QT region depends considerably on the angle between the line of sight and the magnetic field direction being very near 90°, as shown by Chernov and Zlobec (1995). If, for a small spike source, this angle may be 90°, then for a broader total microwave source such an angle is very different for different parts of the broad source and the polarization conversion for the broad source is only partial. That is the reason for a small polarization degree of the total background burst emission. In some cases the interaction of an O-mode with whistlers may contribute to an additional depolarization, if whistlers appear just above the escape level of X-mode.

5. Some Concluding Remarks

A new model for solar spike bursts is considered based on the interaction of Langmuir waves with ion-sound waves: $l + s \rightarrow t$. Such a mechanism can operate in shock fronts, propagating from a magnetic reconnection region in accordance with the simulations of Yokoyama and Shibata (1996) and *Yohkoh* observations of Tsuneta (1996).

New observations of microwave millisecond spikes are discussed. They have been observed in the event of 4 November 1997 between 05:52–06:10 UT and

for the 28 November 1997 event between 05:00–05:10 UT using the multichannel spectrograph in the range 2.6–3.8 GHz of Beijing AO. *Yohkoh*/SXT images in AR for the 4 November event and SOHO EIT images show a reconstruction of bright loops after the escape of a halo CME visible at 06:10 UT with the LASCO C2 coronagraph onboard SOHO.

A fast shock front might be manifested as a very bright line in SXT T_e maps (more than 18 MK) above dense structures in *EM* maps. Moreover, one can see at the moment of spike emission an additional maximum at the loop top on the HXR map in the AR as a main evidence of fast shock propagation.

In such a model one can answer the question: why are spikes observed only episodically during some seconds in each event? The fast shock front crosses the microwave source in some seconds. Moreover, a fast shock wave cannot be formed in all events, but only when the energetic conditions for its formation hold near a flare magnetic loop top, namely when the Mach number $M = V/C_s$ exceeds 1.

Parameters of an individual spike may be determined by the particle acceleration mechanism and by the parameters of narrow shock fronts. A discussion question concerning the small source dimensions of spikes (Altyntsev *et al.*, 1996) is resolved by taking the small bandwidth of the shock front into account.

The model under discussion may be justified by the conclusion of Karlický, Sobotka, and Jiřička (1996) that the narrowband dm-spikes are manifestations of radio emission from electrons accelerated in MHD cascading waves, probably generated in plasma outflows from magnetic field reconnection.

Moreover, our model helps us to propose a new explanation of the observations of decimetric spikes at harmonics $s = 2–6$ (Güdel, 1990). We may relate the emission of consecutive frequency bands of spikes with consecutive magnetic islands with X-point configurations along a vertical magnetic current sheet. Our main remark: millisecond microwave spikes are probably a unique manifestation of flare fast shocks in radio emission.

Acknowledgements

G.P.Ch. is grateful for the support given by the Chinese Academy of Sciences that enabled him to work at BAO. SOHO data used in this paper were received from SOHO Synoptic Data Base, courtesy of SOHO EIT, LASCO, MDI consortiums. G.P.Ch. also wishes to acknowledge the help of J. Newmark, scientist from EIT team and the help of Prof H. Zhang (BAO) for $H\beta$ images. The *Yohkoh* data were provided by the *Yohkoh* mission of ISAS, Japan, which was prepared and is operated by an international collaboration of Japanese, US and UK scientists with the support of ISAS, NASA and PPARC, respectively. *Yohkoh*/HXT data in active regions were provided by courtesy of Dr J. Sato. This work was supported by the National NSF of China and the Chinese Academy of Sciences, by the Russian

Foundation of Basic Research, grant No. 99-02-16076, and by the Russian Federal Program on Astronomy.

References

Allaart, M. A. F. *et al.*: 1990, *Atlas of Fine Structure in Solar Microwave Bursts*, Sterrenkundig Instituut, Utrecht.
Altyntsev, A. T., Grechnev, V. V., Konovalov, S. K. *et al.*: 1996, *Astrophys. J.* **469**, 976.
Altyntsev, A. T., Grechnev, V. V., and Hanaoka, Y.: 1998, *Solar Phys.* **178**, 575.
Aschwanden, M. J.: 1990, *Astron. Astrophys.* **237**, 512.
Aschwanden, M. J. and Güdel, M.: 1992, *Astrophys. J.* **401**, 736.
Benz, A. O.: 1986, *Solar Phys.* **104**, 99.
Benz, A. O.: 1993, *Plasma Astrophysics*, Kluwer Academic Publishers, Dordrecht, Holland.
Benz, A. O. and Güdel, M.: *Solar Phys.* **111**, 175.
Benz, A. O. and Wentzel, D.: 1981, *Astron. Astrophys.* **94**, 100.
Chernov, G. P.: 1990, *Solar Phys.* **130**, 234.
Chernov, G. P. and Fomichev, V. V.: 1989, *Soviet Astron. Lett.* **15**, 410.
Chernov, G. P. and Zlobec, P.: 1995, *Solar Phys.* **160**, 79.
Fleishman, G. D. and Mel'nikov, V. F.: 1998, *Uspehi Fizicheskih Nauk* **168**, 1265.
Fomichev, V. V. and Fainstein, S. M.: 1988, *Soviet Astron.* **65**, 1058 (in Russian).
Fu, Q. J., Gong, Y. F., Jin, S. Z., and Zhao, R. Y.: 1990, *Solar Phys.* **130**, 161.
Güdel, M.: 1990, *Astron. Astrophys.* **239**, L1.
Güdel, M. and Benz, A. O.: 1990, *Astron. Astrophys.* **231**, 202.
Güdel, M. and Zlobec, P.: 1991, *Astron. Astrophys.* **245**, 299.
Gurnett, D. A. *et al.*: 1979, *J. Geophys. Res.* **84**, 2029.
Karlický, M., Sobotka, M., and Jiřička, K.: 1996, *Solar Phys.* **168**, 375.
Krucker, S., Benz, A. O., and Aschwanden, M. J.: 1997, *Astron. Astrophys.* **317**, 569.
Krucker, S., Aschwanden, M. J., Bastian, T. S., and Benz, A. O.: 1995a, *Astron. Astrophys.* **302**, 551.
Krucker, S., Benz, A. O., Aschwanden, M. J., and Bastian, T. S.: 1995b, *Solar Phys.* **160**, 151.
Li, C. S., Fu, Q. J., and Li, H. W.: 1991, *Solar Phys.* **131**, 337.
Melrose, D. B.: 1980, *Plasma Astrophysics*, Gordon and Breach Publishers, New York.
Melrose, D. B.: 1989, *Solar Phys.* **119**. 143.
Melrose, D. B. and Dulk, G. A.: 1982, *Astrophys. J.* **259**, 844.
Melrose, D. B. and Robinson, P. A.: 1994, *Proc. Astron. Soc. Austr.* **11**, 16.
Rabin, D.: 1997, *Solar Phys.* **174**, 281.
Sakai, J.-I. and Ohsava, Y.: 1987, *Space Sci. Rev.* **46**, 113.
Tsuneta, S.: 1996, *Astrophys. J.* **456**, 840.
Tsytovich, V. N.: 1971, *Nonlinear Effects in Plasma*, Plenum, New York.
Tsytovich, V. N.: 1977, *Theory of Turbulent Plasma*, Consultant Bureau, New York.
Wang, D. Y. and Li, D. Y.: 1991, *Solar Phys.* **135**, 393.
Wang, D. Y., Li, D. Y., Fu, Q. J., and Xia, Z. G.: 1997, *Solar Phys.* **246**, 129.
Wentzel, D. and Aschwanden, M. J.: 1991, *Astrophys. J.* **372**, 688.
Wu, C. S.: 1985, *Space Sci. Rev.* **41**, 215.
Yokoyama, T. and Shibata, K.: 1996, *Publ. Astron. Soc. Japan* **48**, 353.
Zheleznyakov, V. V.: 1970 *Radio emission of the Sun and Planets*, Nauka, Moscow.
Zheleznyakov, V. V. and Zaitsev, V. V.: 1975, *Astron. Astrophys.* **39**, 107.
Zheleznyakov, V. V. and Zlotnik, E. Ya.: 1988, *Sov. Astron. Lett.* **14**, 195.